Facile Synthesis and Versatilities of Polyanthraquinoylamine Nanofibril Bundles with Self Stability and High Carbon Yield

Xin-Gui Li[1,2*], Hu Li[1], Mei-Rong Huang[1], & Mark G. Moloney[2]

[1]*Institute of Materials Chemistry, College of Materials Science & Engineering, Tongji University, Si-Ping Road, Shanghai, China.* [2]*Chemistry Research Laboratory, Department of Chemistry, University of Oxford, Mansfield Road, Oxford OX1 3TA, UK.*

These authors contributed equally to this work

A facile synthesis for nanosized conducting polymers with inherent selfstability and multifunctionalities is a main challenge. Here we simply synthesize intrinsically self-stabilized nanofibril bundles of poly(1-anthraquinoylamine) (PAQ) by a template-free method. The critical polymerization parameters were studied to significantly optimize the synthesis, size, properties, and functionalities of the resulted fine nanofibrils with a diameter of ca. 30 nm and length of ~6 μm. The PAQ obtained with ammonium persulfate possesses higher polymerization yield, purer composition, higher conductivity, better melting behaviour, higher thermostability, lower burning enthalpy, and slower degradation than that with other oxidants. Furthermore, the polymer nanofibrils exhibit high self-stability, powerful redispersibility, high purity, and clean surface because of a complete avoidance of the contamination from external stabilizer. The PAQ exhibits widely controllable conductivity moving across ten orders of magnitudes from 10^{-9} to 50 S/cm, photoluminescence, lead-ion adsorbability, very high thermostability in air and extremely high char yield in nitrogen at 1000 °C. These materials would be useful as advanced materials including photoluminescent materials, highly cost-effective carbon precursors, sorbents of toxic metal ions, and cost-efficient conductive nanocomposite with low percolation threshold.

The discovery of nanoscopic conducting polymers with large π-conjugated structures has opened a very important field of modern science[1-3]. Nanostructured conducting polymers are one of the most attractive advanced materials because of a novel combination of their electroconductivity, electroactivity, electrocatalysis, optical activity, heavy metal-ion adsorbability, electrorheology, environmental and thermal stability that have found widely potential applications in the fields of electrical and electronic materials[4], sensors[1,5], enzyme immobilization[6], light emitting diodes[7], electrochromic films[8], transparent conductive films[9], electrorheological fluid[10], and anticorrosion coatings for metals[11]. However, the preparation of nanosized conducting polymers by conventional template polymerizations usually involves a large amount of external template, which leads to impure final nano products.

The conducting polymers containing two or more aromatic rings, such as the polymers from aminoquinoline and diaminonaphthalene, have received a great deal of interest due to their superior multifunctionalities and the optimizable mechanisms by facilely regulating the polymerization and doping conditions[12]. However, poly(1-aminoanthraquinone) (PAQ) has attracted relatively less attention because it is very difficult to synthesize the PAQ with high conductivity. It is reported that poly(1,5-diaminoanthraquinone)[13,14], poly(2-aminoanthraquinone)[15], and poly(1-aminoanthraquinone)[16] have been polymerized, demonstrating some excellent properties, such as good electroactivity, high electrical conductivity, powerful specific electrocapacity, and fast reversible redox ability, and as a result, electroconducting aminoanthraquinone polymers have been investigated for use as electrode materials for biosensors[15,16], secondary batteries, and electrochemical capacitors[13]. Aminoanthraquinone polymers must contain 1,4-benzoquinone groups and the polyaniline(PAN)-like mainchains, which should have higher electroactivity than PAN because of the potential for conjugation of the quinone ($Q/Q^{\bullet -}/Q^{2-}$) with a π-conjugated system[17]. That is to say, a hybridization moiety, for example, quinone ($Q/Q^{\bullet -}/Q^{2-}$) into a

π-conjugated system might give even higher electroactivity than just their simple mixture or the conducting polymer alone. Moreover, the aminoanthraquinone polymer is anticipated as a multifunctional material that will exhibit different properties to conventionally conducting polymers, because the polymer contains 1,4-benzoquinone groups in the aromatic rings as one more redox site than PAN. Therefore, there is no doubt that these novel characteristics of aminoanthraquinone polymers will attract the attention of more scientists from chemistry and materials science.

Here, unexpected fine nanofibrils of PAQ polymers were easily and directly obtained by chemically oxidative polymerization of 1-aminoanthraquinone (AQ) in an acidic organic medium without any external template. The presence of 1,4-benzoquinone groups in PAQ polymers would permit formation and stabilization of the nanofibrils owing to their electrostatic repulsion and steric hindrance effect, thus leading to an *in-situ* fabrication of pure self-stable nanofibril bundles with high purity, high preparation yield, inherent self-stability, adjustable conductivity, extremely high thermostability, and high conducting carbon yield. The significant effect of key polymerization parameters, including the oxidant species, polymerization temperature and time on the yield, structure, and properties of the PAQ nanofibrils has been systematically investigated for the first time.

Synthesis of PAQ nanofibrils

The remarkable dependence of the polymerization yield on the AQ concentration is illustrated in **Figure 1(a)**. As the AQ concentration rises from 0 to 100 mM in $HClO_4/CH_3CN$, the yield of virgin PAQ salt nanofibril bundles demonstrates a maximum of 41.5 % at 50 mM. It is obvious that too low AQ concentration means too few polymerizing active centres, while the polymerizing efficiency at too high AQ concentration was restricted by a limited solubility of AQ in the $HClO_4/CH_3CN$, both of

which result in lower yield. Therefore, the optimal AQ concentration is around 50 mM for the successful synthesis of the PAQ nanofibril bundles.

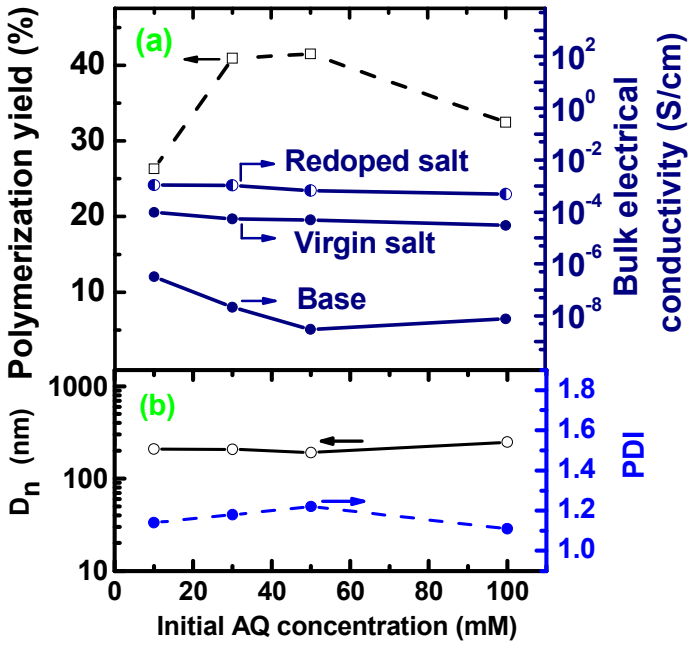

Figure 1 | Effect of AQ monomer concentration on the polymerization yield and bulk electrical conductivity **(a)** and number-average diameter (D_n) and size polydispersity index (PDI) **(b)** of the PAQ salt nanofibril bundles prepared at $(NH_4)_2S_2O_8$/AQ molar ratio of 1 in 50 mM $HClO_4/CH_3CN$ at 0 °C for the polymerization time of 48 h.

The strong effect of the polymerization temperature on the polymerization yield is revealed in **Figure 2(a)**. It can be seen that the yield of the PAQ nanofibril bundles exhibits the maximal value of 74.3% at 15 °C. As the polymerization temperature is elevated from 15 to 50 °C, the yield gradually decreases to the lowest value, possibly due to the loss of more oligomers formed at higher temperature. Too high temperature would induce more chain termination, whereas too low temperature might cause slower and less chain initiation and propagation. The chemical oxidative polymerization of aniline and 4-sulfonic diphenylamine shows a similar relationship between polymerization temperature and yield[18]. It is concluded that 15 °C is the most favorable

temperature for the AQ polymerization because it gives the highest yield of PAQ, which should be attributed to the proper chain initiation and propagation rates.

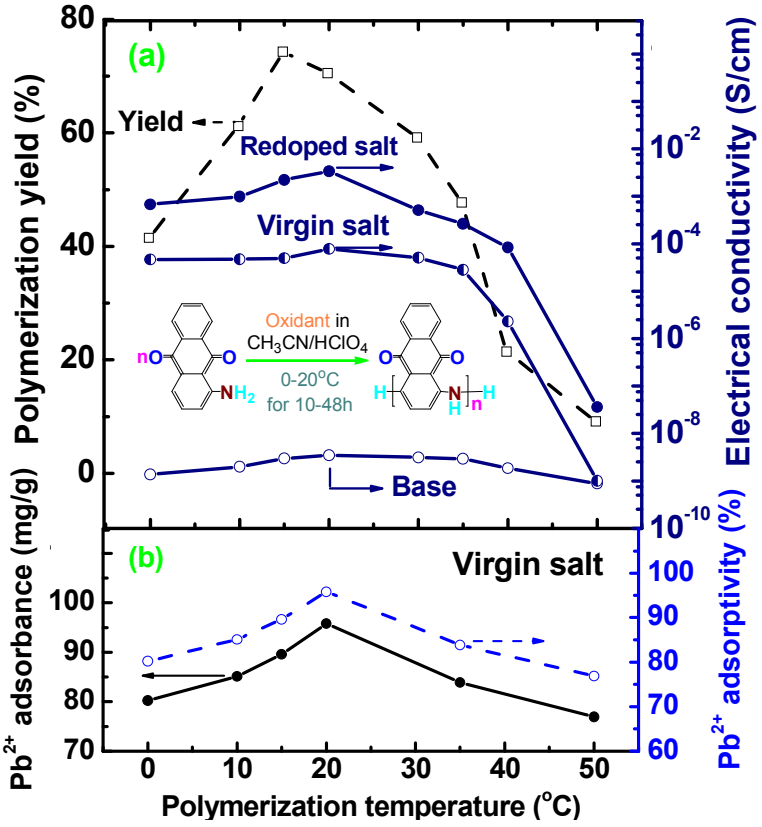

Figure 2 | Influence of polymerization temperature on **(a)** polymerization yield and bulk electrical conductivity and **(b)** adsorbance and adsorptivity of Pb^{2+} of PAQ nanofibril bundles prepared by a chemically oxidative polymerization (**inset**) at a fixed $(NH_4)_2S_2O_8$/AQ molar ratio of 1 and initial AQ concentration of 50 mM in 50 mM $HClO_4/CH_3CN$ for 48 h with different polymerization temperatures in 25 mL $Pb(NO_3)_2$ solution at initial Pb^{2+} concentration of 200 mg/L at 30°C for adsorption time of 24 h.

Structure of the PAQ nanofibrils

The IR spectra of AQ monomer and PAQ nanofibril bundle bases obtained with different oxidants and polymerization temperatures are shown in **Figure S3**. A strong doublet due to -NH_2 stretching at approximately 3430 and 3310 cm^{-1} in the spectrum of

AQ monomer has turned into a broad singlet centered at around 3450 cm^{-1} in three spectra of PAQs, which strongly suggests that almost all of the free -NH_2 groups in the monomer have changed to -NH- groups after the polymerization. The three types of PAQ polymers oxidized by three oxidants exhibit basically similar IR spectra, indicating similar chain structures, but only PAQ obtained by $(NH_4)_2S_2O_8$ exhibits a stronger peak at 1580 cm^{-1} to quinoid rings than at 1490 cm^{-1} to benzenoid rings, implying a higher content of the quinoid rings in the polymer. The UV-vis absorption spectra of all PAQ salts in **Figure S4** exhibit three bands: the first band at 260-280 nm owing to a π-π* transition[19,20], the second band at 420-460 nm due to quinone groups, and the third band centered at 600-650 nm due to an n-π* excitation band from the benzenoid to the quinoid ring in the polymer chains[21], which are quite different from the UV-vis spectra of the AQ monomer. The strong band of the monomer centered at 380-480 nm due to quinone groups has become a moderate or even weak band for the three PAQs[22]. Moreover, the PAQs display a unique band at 600-670 nm corresponding to the excitation of the large π-conjugated system in their PAN-like units,[17] but this band was not observed in the UV-vis spectra of AQ monomer. The wide-angle X-ray diffractograms for virgin salts of the PAQ polymers obtained with three oxidants in **Figure 3** suggest that the polymers are substantially amorphous, that is quite different from the AQ monomer with highly crystalline structure (top curve in **Figure 3**). The PAQs show four diffraction peaks at the Bragg angle 2θ of 8.9°, 12.6°, 18.4° and 25.8°. The two strongest peaks centered at 12.6° and 25.8° should be attributed to the periodicity parallel and perpendicular to the PAN-like mainchains, respectively[23]. The PAQ obtained by H_2O_2/Fe^{2+} appears to be the most amorphous and exhibits nearly the same intensity of the peaks at ca. 3° and 25°, suggesting a presence of larger ordered sizes. Although all of three polymers is low crystalline, the PAQ oxidized by $(NH_4)_2S_2O_8$ is the most crystalline. In short, very different IR/UV-vis spectra and X-ray diffractograms between the monomer and the oxidative products strongly indicate that

the oxidative products are real polymers rather than a simple complex or mixture of monomers with some oligomers.

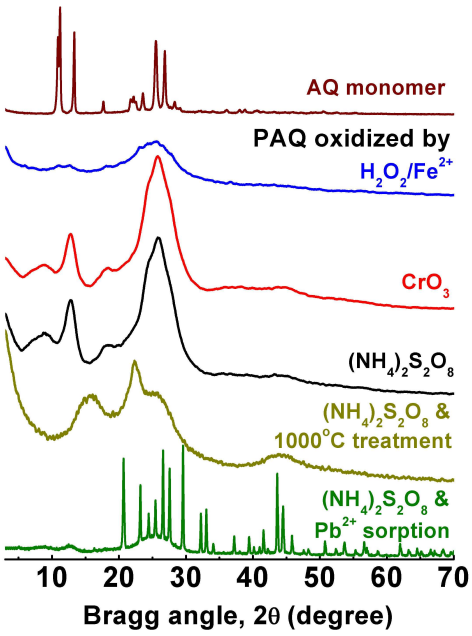

Figure 3 | X-ray diffractograms of AQ monomer and PAQ salt nanofibril bundles prepared with the oxidant/AQ molar ratio of 1 in 50 mM $HClO_4/CH_3CN$ at 15 °C for 48 h. Thermal treatment: the PAQ obtained with the oxidant of $(NH_4)_2S_2O_8$ was heated from 20 to 1000°C at 40°C/min under N_2. Pb^{2+} sorption: 50mg PAQ obtained with $(NH_4)_2S_2O_8$ in 25 mL 200 mg/L $Pb(NO_3)_2$ solution at 30°C for 24 h.

Size and morphology of the PAQ nanofibril bundles

The size and morphology of the PAQ nanofibrils fabricated with $(NH_4)_2S_2O_8$ in 50 mM $HClO_4/CH_3CN$ solution at 20 °C for 48 h were analyzed by TEM and SEM techniques in **Figure 4**. The PAQ nanofibrils appear to gather into clusters. In **Figure 4(a,c)**, a great amount of nanofibrils have the diameter of around 10-50 nm, which interpenetrate with each other and become a single nanofibril bundle. The SEM images in **Figure 4(b, d)** reveal that the PAQ nanofibrils exhibit a mean diameter of around 60 nm in a range from 30 to 90 nm. The size of the nanofibrils revealed by TEM is smaller than that by

SEM because of the gold sputter coating prior to SEM observation. The PAQ polymerized at 15 and 0 °C can also form the nanofibril bundles, as shown in **Figures 4-5**. These nanofibrils look more irregular than those synthesized at 20 °C.

It is interesting that the stable PAQ nanofibril colloids can clearly be observed when as-formed nanofibril bundles are washed and purified with water by centrifugation. The dispersion gradually becomes darker as the nanofibrils become purer with increasing number of washing/centrifugation cycles. After three cycles of washing-centrifugation, the whole dispersion remains dark blue even after centrifugation at 3400 rpm for 20 min or longer, indicating that stable PAQ nanofibril colloids have formed because of stabilization through electrostatic repulsion. The size and its distribution of the PAQ nanofibril colloids have been shown in **Figures 1(b), S5 and S6**. The AQ concentration and polymerization medium show a slight effect on the size and its polydispersity of the PAQ colloids, but the polymerization temperature and time show much stronger effect. Only the polymerization at 0-20 °C for 48-72 h could provide the PAQ colloids with number-average diameter of around 200 nm and size polydispersity index of 1.2. A similar phenomenon has been observed in the formation of other conducting polymer nanofibrils[24]. It is apparent that the self-stabilization of the nanofibrils would be assigned to the existence of negatively charged quinone groups on the polymer units. The quinone group as an internal stabilizer can provide strong static repulsion and steric hindrance amongst the nanofibrils and thus efficiently stabilize them. On the other hand, the polymer mainchains have a tendency to force the nanofibrils to grow along the axial direction of nanofibrils because of the high rigidity of the PAQ polymer mainchains (see **Figure 2**). Therefore, the nanofibrils with high purity and clean surface can facilely be obtained here because 1) no external stabilizer was added into the polymerization medium and 2) dissociative HCl, residual AQ monomer and oxidant, and its reducing product $(NH_4)_2SO_4$ in or on the nanofibrils have been totally removed by centrifugation in water.

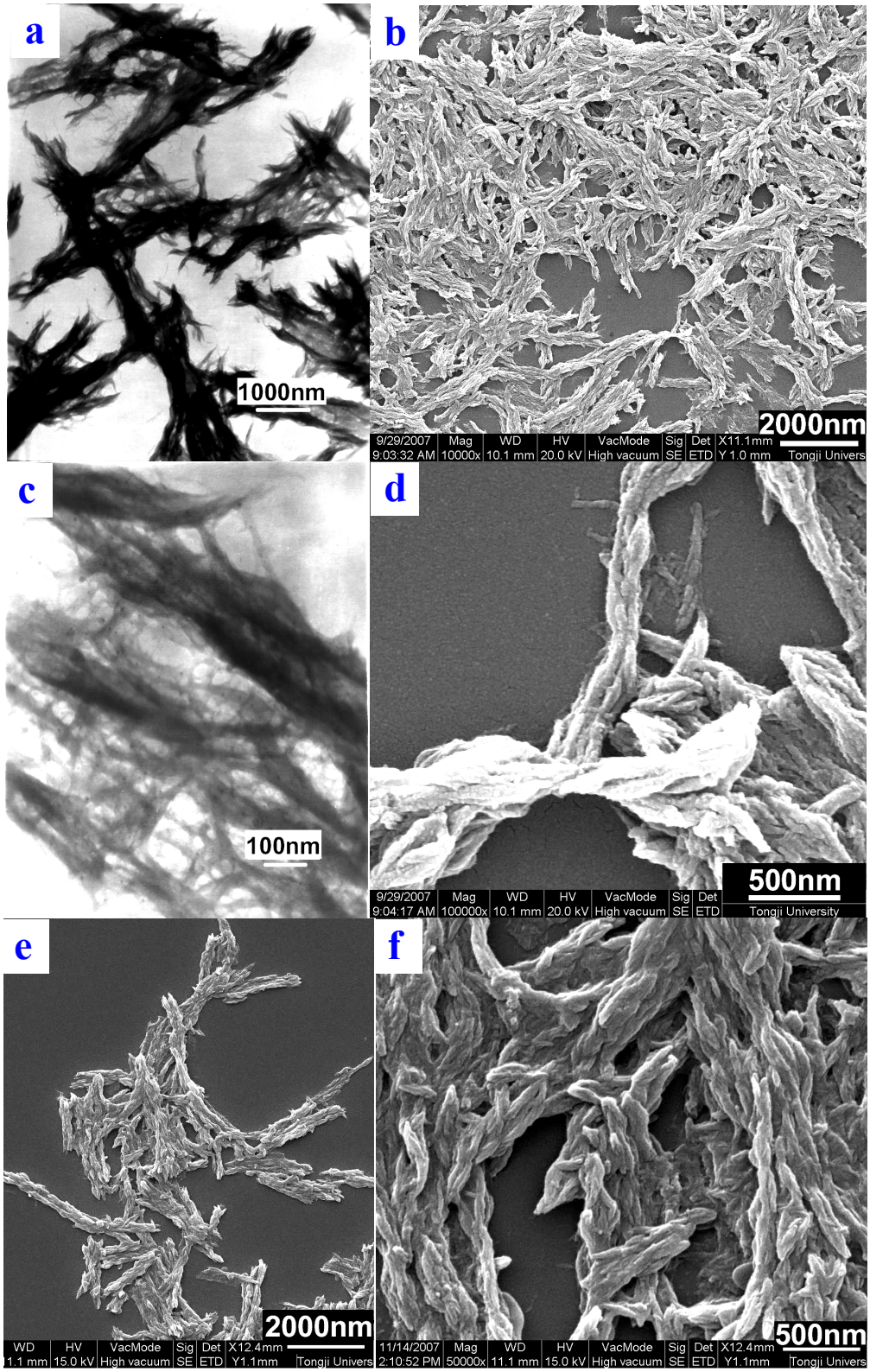

Figure 4 | Different magnification TEM(**a,c**) and SEM(**b,d,e,f**) images of PAQ nanofibrils prepared with $(NH_4)_2S_2O_8$/AQ molar ratio of 1 in 50 mM $HClO_4$ in CH_3CN at 20 °C(**a-d**) and 15 °C(**e,f**) for 48 h.

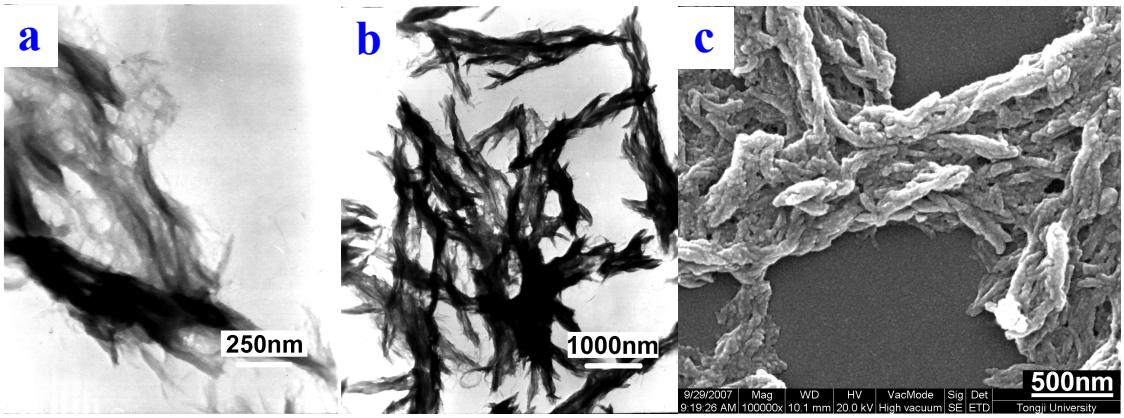

Figure 5 | TEM(**a,b**) and SEM(**c**) images of PAQ nanofibril bundles prepared with $(NH_4)_2S_2O_8$/AQ molar ratio of 1 in 50 mM $HClO_4$ in CH_3CN at 0 °C for 48 h.

Properties of the PAQ nanofibril bundles

Bulk electrical conductivity of the PAQ nanofibril bundles strongly depends on the polymerization conditions like AQ concentration, oxidant species, polymerization temperature and time. As illustrated in **Figure 1(a)**, the redoped salts of PAQ formed at an AQ concentration of 100 mM possess higher conductivity corresponding to lower yield, but the redoped salts of PAQ formed at an AQ concentration of 50 mM possess the lowest conductivity corresponding to the highest yield. That is to say, the yield is inversely proportional to the conductivity with the AQ concentration for the polymerization. As summarized in **Table S1**, the electrical conductivity of the PAQs significantly changes with oxidant species. The PAQ formed with $(NH_4)_2S_2O_8$ exhibits the highest conductivity(2.2×10^{-3} S/cm), but the PAQ formed with H_2O_2/Fe^{2+} shows the lowest conductivity. This phenomenon compares with the results of IR and UV/vis spectra, WAXD, and solubility (**Figures S3, S4, 3, and Table S1**). Furthermore, the conductivity varies dramatically in a wide range from 10^{-10} to 10^{-3} S/cm with changing oxidant species with various standard reduction potentials. Apparently, H_2O_2/Fe^{2+} is the worst oxidant but $(NH_4)_2S_2O_8$ is the best for the productive synthesis of highly conducting PAQ nanofibrils. This indicates that the standard reduction potentials of the oxidant plays an important role in the formation of the large π-conjugated mainchains of

the polymers. In particular, the conductivity of the PAQ polymers obtained depends remarkably on the polymerization temperatures (**Figure 2**). The most important finding is that the conductivity reaches a maximum (3.36×10^{-3} S/cm) at the polymerization temperature of 20 °C. A monotonically decreased conductivity of the polymers with further elevating polymerization temperature from 20 to 50 °C can be ascribed to the formation of more polymers with short π-conjugation length. Besides, polymerization time is another important factor influencing the conductivity of the PAQ polymers (**Figure S2**). A maximum conductivity appeared at the polymerization time of 48 h when $(NH_4)_2S_2O_8$ was used as the oxidant at a fixed oxidant/monomer ratio of 1 in 1 M $HClO_4/CH_3CN$ solution at 20 °C. Normally, increasing polymerization time would lead to greater molecular mass and longer π-conjugated length of polymers, which will finally improve their conductivity. However, the conductivity of PAQs declines after the polymerization time over 48 h, possibly due to the secondary reaction of grafting onto the main chains after a certain degree of polymerization. After a comparison of conductivity-time relations, it seems that 48 h is the optimal polymerization time for the synthesis of the PAQ nanofibrils with the highest conductivity. The conductivity of the redoped PAQ salt formed with CrO_3 as oxidant at 15 °C also displays a maximum of 2.4×10^{-4} S/cm at the polymerization time of 48 h. The enhanced chromic ion adsorbance onto the PAQ nanofibrils should be responsible for the lowered conductivity from 2.4×10^{-4} to 5.24×10^{-5} with increasing polymerization time from 48 to 96 h. It seems that the oxidative polymerization for chain propagation has stopped after 48 h. Note that the dependency of the conductivity on the polymerization time is different if the polymerization temperature was lowered to 15 to 0 °C with $(NH_4)_2S_2O_8$ as the oxidant. Therefore, the conductivity is very sensitive to the polymerization and doping conditions because the redox-state, doping state, molecular weight, and π-conjugation length of the PAQs are dramatically influenced by polymerization conditions. In other

words, the conductivity could be efficiently optimized by controlling and regulating the polymerization and doping conditions.

Photoluminescent characteristics including the excitation and emission spectra of the AQ monomer and PAQ nanofibrils in several media are shown in **Figure 6**. It is found that all excitation spectra exhibited a strong band between 230 nm and 350 nm corresponding to $\pi \rightarrow \pi^*$ electronic transitions. The triple bands in NMP as solvent are characteristic of many π-conjugated polymers and arise from a distribution of large π-conjugation lengths. The emission spectra, which are assigned to the radiative decay of excitons, have a more pronounced vibronic structure, exhibiting a maximum between 330 and 412 nm. Note that the shape, position and intensity of the excitation and emission spectra of PAQ polymers differ significantly from those of the AQ monomer. The excitation and emission intensities of the PAQ in NMP due to fluorescence reinforcement by PAN-like π-conjugated chains are much stronger than those of AQ monomer of the same concentration in NMP. This phenomenon reflects the fact that the PAQ has quite different molecular structure from the AQ monomer, which is a real π-conjugated electroconducting polymer.

Some excitation and emission peaks in **Figure 6** were blue or red shifted accompanied by changes of their luminescent intensity, depending on the medium employed. The excitation and emission are greatly affected by solvent polarity which can modulate the fundamental and excited states of the polymer. Media of high polarity would stabilize the excited state with a highly polar character on a low energy level, causing a red-shift of the emission. A blue shift is expected for solvents of low polarity. Therefore, the photoluminescence of the PAQ is dependent upon the medium around it. The luminescent emission maximum of the PAQ dispersion shifts to longer wavelengths from 302 to 358 nm as the dielectric constant of the medium increases from 25(ethanol) to 80(water). The PAQ solution in NMP (**Figure 6**) presents three excitation bands at 274/314/350 nm and two emission bands at 356/412 nm. In comparison with the PAQ

solution in NMP, the PAQ nanofibril dispersions in ethanol and water show very weak and blue-shifted fluorescence bands. However, the PAQ nanofibrils exhibit the strongest fluorescence band at 347 nm if dispersed in 0.1 M DBSA aqueous solution. These results indicated that the dispersion state and microenvironment of the PAQ nanofibrils significantly influence the fluorescence properties. It is known that nanosized conducting polymers would produce a nanoeffect, shortening π-conjugated bond length and then leading to the localization of free electrons due to some lattice defects. But, the PAQ nanofibrils should have an expanded or "open" configuration when dispersed in the DBSA micelle solution because of the strong interaction between the micelle molecules and the functional imino groups on PAQ nanofibrils.

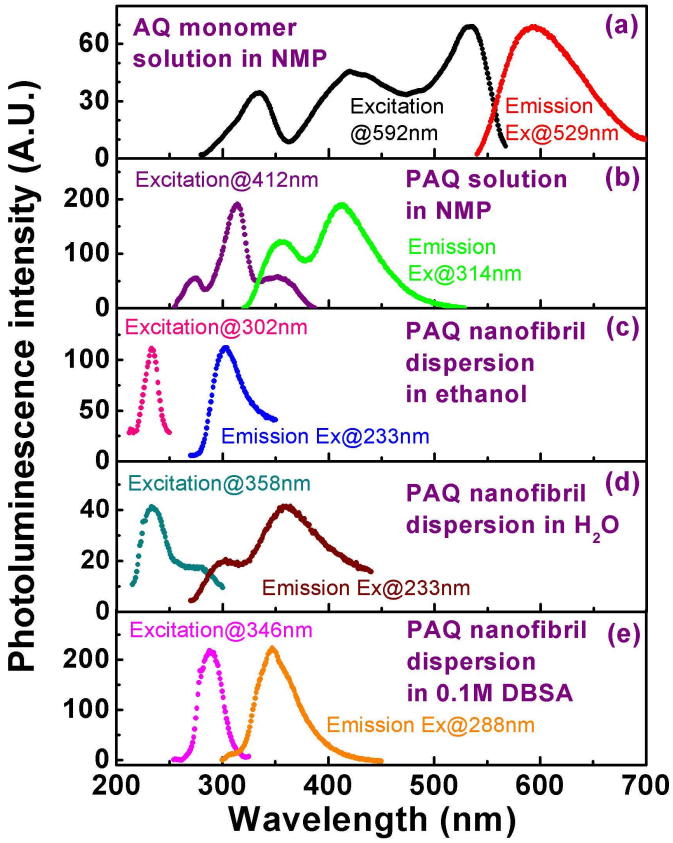

Figure 6 | Excitation and emission scans for AQ solution in NMP (**a**) and PAQ nanofibrils dissolved in NMP (**b**), and dispersed in ethanol (**c**), water (**d**), and 0.1 M DBSA aqueous solution (**e**), at the same concentration of 10 mg/L.

Pb^{2+} adsorbance and adsorptivity onto the PAQ nanofibrils first increase first and then decrease with polymerization temperature rise from 0 to 50 °C in **Figure 2(b)**, displaying the maximal adsorbance and adsorptivity at 20 °C, possibly due to the presence of the most -N= groups in the chains of PAQ synthesized at 20 °C. The decreased content of –N= groups on the PAQs at lower or higher temperature has been revealed by the IR and UV/vis spectral results as discussed above (**Figures S3 and S4**). In short, the PAQ fine nanofibrils synthesized at 20 °C possess the second highest polymerization yield, the highest conductivity, the longest UV/vis absorbance wavelength, and the strongest Pb^{2+} adsorbability.

The occurrence of Pb^{2+} adsorption onto the PAQ nanofibrils has been further confirmed by the variation of the wide-angle X-ray diffractogram of the nanofibrils adsorbing Pb^{2+}(**Figure 2**). The PAQ salts adsorbing Pb^{2+} display a series of new sharp diffraction peaks (bottom curve in **Figure 3**) as compared with the original salts, indicating the existence of $PbSO_4$ from a reaction between Pb^{2+} and SO_4^{2-} groups as the dopant. This phenomenon is similar to the Pb^{2+} sorption onto poly(*m*-phenylenediamine) microparticles[25], implying that the chelation and precipitation sorptions of Pb^{2+} onto the PAQ salts occur simultaneously. Furthermore, the Pb^{2+} sorption of PAQ nanofibrils could be attributable to a chelation between Pb^{2+} ions and the -N= groups through sharing the four lone pairs of electrons on the four nitrogen atoms[26,27]. In addition, other possible routes for the Pb^{2+} sorption could be an ion exchange of Pb^{2+} ions on the protonated -N= groups and the reduced quinone groups of polymer chains. Especially, the PAQ exhibits much stronger Pb^{2+} adsorbability than poly(diaminoanthraquinone). Under the same sorption condition, the poly(diaminoanthraquinone) synthesized with oxidant (CrO_3)/monomer (diaminoanthraquinone) molar ratio of 1/1 at a polymerization temperature of 0 °C for 24 h has low Pb^{2+} adsorbance of 37.0 mg/g and Pb^{2+} adsorptivity of 37.9%, suggesting obviously different macromolecular structures.

DSC scans of the PAQs synthesized with three oxidants at 0, 15 and 20 °C all show an endothermic peak centered at 70-90 °C due to the evaporation of water trapped inside the polymers (**Figure 7(DSC) inset)**. In addition, respective strong and medium exothermic peaks at 264 and 361 °C were observed for the PAQ oxidized by CrO_3, possibly due to a series of complicated chemical reactions like crosslinking. The PAQ oxidized by H_2O_2/Fe^{2+} displays very weak exothermic peaks at 244 and 309 °C. On the contrary, three PAQs oxidized by $(NH_4)_2S_2O_8$ at 0, 15, and 20 °C exhibit weak endothermic peaks at 325, 331, and 330 °C, respectively, probably originating from the melting of the polymers. This means that the PAQs oxidized by CrO_3 and H_2O_2/Fe^{2+} are thermally instable compared to the PAQs oxidized by $(NH_4)_2S_2O_8$ because the former has lower molecular weight and more impurities such as chromic or ferric/ferrous active ions, which was further confirmed by the following TG study in air.

Figure 7 shows simultaneous TG and DSC curves of PAQs in air and nitrogen. The polymers show a two-step weight-loss behaviour in air. The first step is a 10-20% weight loss at 200-530 °C, which is likely to be caused by the exclusion of the residual dopant, oxidants and their reduced products trapped in the samples, the quinone and end-amino groups. The second-step major weight loss, accompanied by an obvious exothermicity, is attributed to the decomposition of the polymer backbones. It is surprisingly noted that the PAQ oxidized by $(NH_4)_2S_2O_8$ at 15°C exhibits an extremely high thermostability in air. The degradation of PAQ main chain occurs up to 550 °C, and the temperature corresponding to the maximal weight-loss rate of only 0.8 %/min dramatically increased to 625°C. Apparently, the PAQ nanofibrils obtained with $(NH_4)_2S_2O_8$ as the oxidant possess much better melting behaviour, much higher thermostability, much smaller burning enthalpy, much slower degradation, and much lower char yield at 1000°C than those with CrO_3 and H_2O_2/Fe^{2+}, indicating that the PAQ obtained with $(NH_4)_2S_2O_8$ has higher molecular weight and much purer composition because there should be impurity like chromic and ferrous compounds in

the PAQ obtained with the latter two oxidants. It seems that this PAQ is more thermostable in air than most other highly heat-resistant polymers, except for wholly aromatic polyimide[28], poly(3-ethynylphenanthrene)[29] and poly(*p*-phenylene benzobisoxazole)[30] with very high cost in **Table S2**. That is to say, the PAQ appears to be a highly thermostable cost-effective polymer owing to a combination of its high aromaticity and good π-conjugated structure of polycyclic fused ring type.

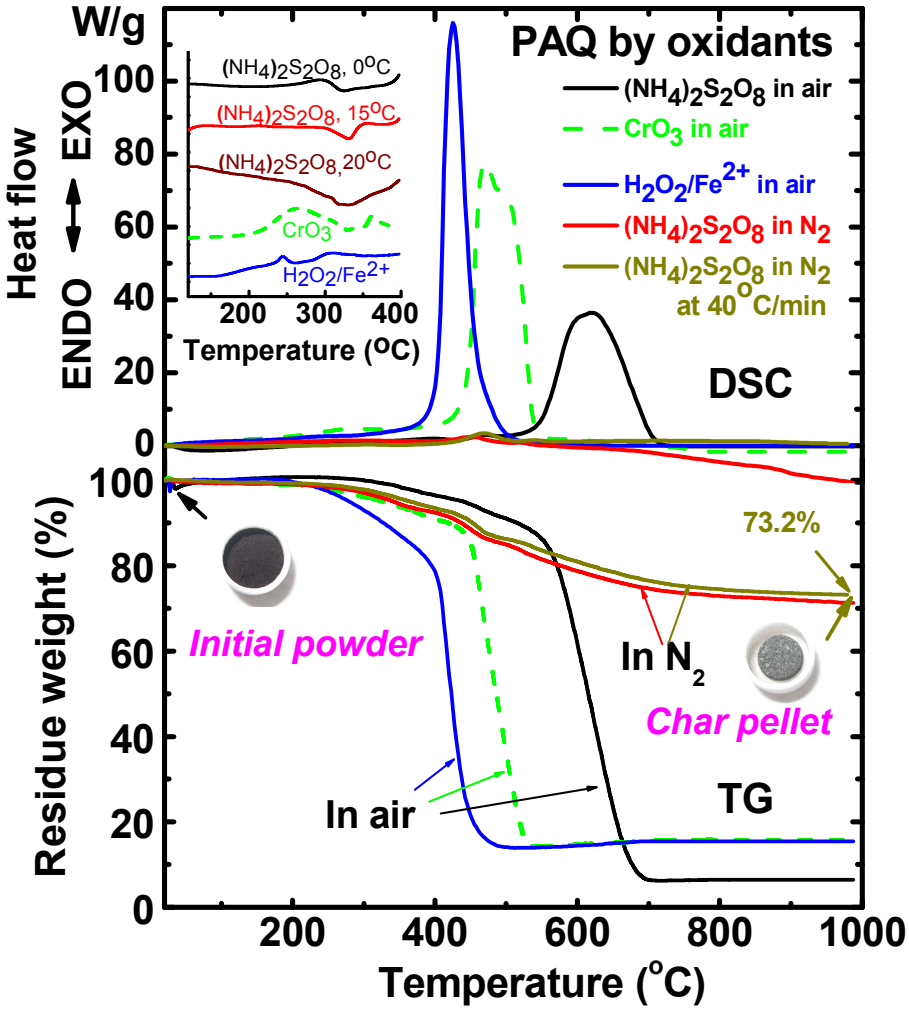

Figure 7 | DSC and TG thermograms in air and nitrogen of dedoped PAQ bases obtained with three oxidants at a fixed oxidant/AQ molar ratio of 1 in 50 mM $HClO_4/CH_3CN$ at 15 °C for 48 h. Upper left inset: DSC thermograms in nitrogen of as-polymerized PAQ bases obtained by $(NH_4)_2S_2O_8$ were synthesized at 0, 15, 20 °C.

Furthermore, it was surprisingly discovered that the PAQ powders oxidized by $(NH_4)_2S_2O_8$ at 15°C exhibit an extremely high char yield in nitrogen(**Table S2**). After a slow weight loss of, at the utmost, 0.1%/min, at relatively low temperature of 310 to 460 °C, a black pellet char yield at 1000 °C is up to 71.3-73.2 %, that is 93.8-96.3% of the theoretical char yield of 76.0%. The residual char pellet exhibits different X-ray diffraction (the 2nd curve from the bottom in **Figure 3**), different density (0.9 g/cm^3) but much higher conductivity (50 S/cm) than the starting PAQ base powders (3×10^{-9} S/cm in **Figure 2**) because the shaggy PAQ base powders (19.7 mg) in the ceramic crucible have converted or shrunk into porous char pellet with a weight of 14.4 mg, a diameter of 4.1 mm and thickness of 1.2 mm (inset of **Figure 7(TG))** after an efficient melting and felting at an elevated temperature from 25 to 1000 °C. This suggests that PAQ could be a valuable new carbon precursor because it can be facilely synthesized in acidic CH_3CN/water at ambient temperature/pressure with low-cost dye-intermediate AQ as direct monomer and then carbonized at a low temperature of around 450°C in nitrogen, but still achieve a higher carbon yield than most traditional flame-retardant polymers, except for two ethynyl polymers[31,32] and poly(*p*-phenylene)[33]. The latter have an extremely high cost and complicated synthetic process as shown in **Table S2**. This char could act as an insulative shield when burning, protecting underlying substrates. The PAQ nanofibrils synthesized here represent significant progress in the development of advanced materials, because it offers a good combination of unique heat and flame resistance and high char yield with simple synthetic route and low cost.

Conductive nanocomposite film of the PAQ nanofibrils

Figure S7 reveals that the electroconductivity of PVA nanocomposite films containing the PAQ nanofibrils rises dramatically from 2.14×10^{-14} to 1.55×10^{-5} S/cm with increasing the nanofibril content from 0 to 5.0 wt%. The method based on the scaling law of percolation theory yields a percolation threshold value of 0.1 wt% and a critical exponent of 1.86 that is in well agreement with the predicted universal value (t = 1.7~2

for three-dimensional blend system)[36]. This percolation threshold is significantly lower than that of nanocomposite films of PAN nanofibrils in polymethyl methacrylate,[9] because of a unique ability for the PAQ nanofibrils with a great aspect ratio to connect with each other to form an electrically conductive nanochannel or nanonetwork of effectively conducting electricity, as shown in **Figures 4-5**.

Conclusions

A new class of intrinsically conducting polymer nanofibrils was successfully synthesized by a facile oxidative polymerization of AQ monomer in an organic acidic medium in the absence of any external template. Five key synthetic parameters involving the monomer concentration, polymerization medium, oxidant species, polymerization temperature and time have been optimized for the formation of fine PAQ nanofibrils with high polymerization yield, fine fibril size, and optimal properties including conductivity, Pb^{2+} sorbability, and thermostability. The presence of quinone groups on the polymer chains is vital for the formation and self-stabilization of the nanofibrils with the diameter as small as 30 nm by means of the oxidative polymerization of AQ monomer. The quinone groups act as a unique internal stabilizer that can engender strong electrostatic repulsion between the as-formed nanofibrils. The polymer nanofibrils are good semi-conductors with widely adjustable conductivity, either by facilely regulating the polymerization parameters, or by reversible acid doping/alkali dedoping or by heat treatment, giving a range of conductivity from 10^{-9} to 50 S/cm. The polymers exhibit good solubility in polar solvents like concentrated H_2SO_4 and NMP but good chemical resistance in strong acid/alkali solution. A strong fluorescence emission was observed from the PAQ nanofibril dispersion and its NMP solution. The nanocomposite film of the PAQ nanofibrils in PVA exhibits a low percolation threshold of 0.1 wt%, and the nanofibrils easily form nano-channels or -networks which are efficient electrical conductors. With increasing nanofibril loading

from 0 to 5.0 wt%, the conductivity of the derived nanocomposites increases drastically from 2.14×10^{-14} to 1.55×10^{-5} S/cm. These endow the nanofibrils with a wide potential application as photoluminescent and semi-conducting materials, and powerful Pb^{2+} sorbent for recovery and elimination of harmful heavy metal ions from waste water. In particular, the PAQ is a highly heat- and fire-resistant material with an extremely high char yield of 73.2 % in nitrogen and very high cost efficiency because of its very cost-effective synthetic route and low cost of monomer.

METHODS SUMMARY

The PAQ nanofibrils were prepared by a chemical oxidative polymerization of AQ monomer. A typical polymerization procedure is as follows: 40 mL of 50 mM $HClO_4$ in CH_3CN containing a very small amount of water in a 150 mL glass flask in a water bath at 20 °C was added 446 mg (2 mmol) AQ and then stirred vigorously for half an hour. An oxidant solution was prepared separately by dissolving 456 mg (2 mmol) $(NH_4)_2S_2O_8$ in 1 mL deionized water. The AQ solution was then treated with the $(NH_4)_2S_2O_8$ solution by dropwise adding the $(NH_4)_2S_2O_8$ solution at a rate of one drop (around 60 μL) per 20 sec. The reaction mixture was stirred continuously at 20 °C for 48 h together with an *in-situ* measurement of the open-circuit potential (OCP) and temperature of the polymerization solution. After that, the polymer precipitates as virgin salts were isolated from the reaction mixture by filtration and washed with ethanol and an excess of distilled water in order to remove the remaining monomer, oxidant and its reduced product ($-SO_4^{2-}$) and soluble oligomers until no $BaSO_4$ precipitate was detected after adding 1 mM $BaCl_2$ aqueous solution. A part of the PAQ salt was subsequently stirred and neutralized in 100 mL of 0.2 M NH_4OH for 24 h for the preparation of PAQ dedoped base. On the other hand, the PAQ virgin salts were further redoped in 1 M $HClO_4$ aqueous solution for 24 h for the preparation of redoped salt samples. All the resultant polymers were left to dry in ambient air for 3 days, obtaining the PAQ salt and base as fine dark blue powders.

1. Jang, J., Ha, J. & Cho, J. Fabrication of water-dispersible polyaniline-poly(4-styrenesulfonate) nanoparticles for inkjet-printed chemical-sensor applications. *Adv. Mater.* **19**, 1772-1775 (2007).
2. Nikiforov, M., Liu, H. Q., Craighead, H. & Bonnell, D. Polarization controlled transport in PANI-$BaTiO_3$ nanofibers. *Nano Lett.* **6**, 896-900 (2006).
3. Gewin, V. Nanotech's big issue. *Nature* **443(7108)**, 137-137 (2006)
4. Winther-Jensen,B., Winther-Jensen, O., Forsyth, M.& MacFarlane, D. R. High rates of oxygen reduction over a vapor phase-polymerized PEDOT electrode. *Science* **321(5889)**, 671-674 (2008).
5. Bekyarova, E., Kalinina, I., Itkis, M. E., Beer, L., Cabrera, N. & Haddon, R. C. Mechanism of amonia detection by chemically functionalized single-walled carbon nnotubes: in situ electrical and optical study of gas analyte detection. *J. Am. Chem. Soc.* **129**, 10700-10706 (2007)
6. Rumbau, V., Marcilla, R., Ochoteco, E., Pomposo, J. A. & Mecerreyes, D. Ionic liquid immobilized enzyme for biocatalytic synthesis of conducting polyaniline. *Macromolecules* **39**, 8547-8549 (2006).
7. Yang, C. H. & Chih, Y. K. Molecular assembled self-doped polyaniline interlayer for application in polymer light-emitting diode. *J. Phys. Chem. B* **110**, 19412-19417 (2006).
8. DeLongchamp, D. M. & Hammond, P. T. High-contrast electrochromism and controllable dissolution of assembled prussian blue/polymer nanocomposites. *Adv. Funct. Mater.* **14**, 224-232 (2004).
9. Wang, Y. Y. & Jing, X. L. Transparent conductive thin films based on polyaniline nanofibers. *Mater. Sci. Eng. B* **138**, 95-100 (2007).
10. Park, J. H., Lim, Y. T. & Park, O. O. New approach to enhance the yield stress of electro-rheological fluids by polyaniline-coated layered silicate nanocomposites. *Macromol. Rapid Commun.* **22**, 616-619 (2001).
11. Zhang, D. H. Preparation of core-shell structured alumina-polyaniline particles and their application for corrosion protection. *J. Appl. Polym. Sci.* **101**, 4372-4377 (2006).
12. Freire, J. A., Dal Moro, G. A., Toniolo, R., Hummelgen, I. A. & Ferreira, C. A. Polymeric electronic oscillators based on bistable conductance devices. *Org. Electron.* **7**, 397-402 (2006).

13. Naoi, K., Suematsu, S., Hanada, M. & Takenouchi, H. Enhanced cyclability of π-π stacked supramolecular (1,5-diaminoanthraquinone) oligomer as an electrochemical capacitor material. *J. Electrochem. Soc.* **149**, A472-A477 (2002).

14. Li, X. G., Li, H. & Huang, M. R. Productive synthesis and properties of polydiaminoanthraquinone and its pure self-stabilized nanoparticles with widely adjustable electroconductivity. *Chem. Eur. J.* **13**, 8884-8896 (2007).

15. Ju, H. X., Sun, H. B. & Chen, H. Y. Properties of Poly-β-aminoanthraquinone modified carbon fiber electrode as a basis for hemoglobin biosensors. *Anal. Chim. Acta* **327**, 125-132 (1996).

16. Badawy, W. A., Ismail, K. M. & Medany, S. S. Optimization of the electropolymerization of 1-amino-9,10-anthraquinone conducting films from aqueous media. *Electrochim. Acta* **51**, 6353-6360 (2006).

17. Naoi, K., Suematsu, S. & Manago, A. Electrochemistry of poly(1,5-diaminoanthraquinone) and its application in electrochemical capacitor materials. *J. Electrochem. Soc.* **147**, 420-426 (2000).

18. Li, X. G., Zhou, H. J., Huang, M. R., Zhu, M. F. & Chen, Y. M. Facile synthesis and characterization of the copolymers and their pure nanoparticles from aniline with sulfonic diphenylamine. *J. Polym. Sci. Part A: Polym. Chem.* **42**, 3380-3394 (2004).

19. Nguyen, M.T., P. Kasai, J.L. Miller, & A.F. Diaz, Synthesis and properties of novel water-soluble conducting polyaniline copolymers. *Macromolecules* **27**, 3625-3631 (1994).

20. Li, X. G., Q. F. Lu, Huang, M. R. Facile synthesis and optimization of conductive copolymer nanoparticles and nanocomposite films from aniline with sulfodiphenylamine. *Chem. Eur. J.* **12**, 1349-1359 (2006).

21. Wei, W., Focke, W. W., Wnek, G. E., Ray, A. & MacDiarmid, A. G. Synthesis and electrochemistry of alkyl ring-substituted polyanilines. *J. Phys. Chem.* **93**, 495-499 (1989).

22. Yamamoto, T. & Etori, H. Poly(anthraquinone)s having a π-conjugation system along the main chain. synthesis by organometallic polycondensation, redox behavior, and optical properties. *Macromolecules* **28**, 3371-3379 (1995).

23. Chaudhari, H. K. & Kelkar, D. S. X-ray diffraction study of doped polyaniline. *J. Appl. Polym. Sci.* **62**, 15-18 (1996).

24. Li, D. & Kaner, R. B. Processable stabilizer-free polyaniline nanofiber aqueous colloids. *Chem. Commun.* 3286-3288 (2005).

25. Huang, M. R., Peng, Q. Y. & Li, X. G. Rapid and effective adsorption of lead ions on fine poly(phenylenediamine) microparticles. *Chem. Eur. J.* **12**, 4341-4350 (2006).

26. Jin, L. & Bai, R. Mechanisms of lead adsorption on chitosan/PVA hydrogel beads. *Langmuir* **18**, 9765-9770 (2002).

27. Gupta, R. K., Singh, R. A. & Dubey, S. S. Removal of mercury ions from aqueous solutions by composite of polyaniline with polystyrene. *Sep. Purif. Technol.* **38**, 225-232 (2004).

28. Li, X. G., Huang, M. R., Bai, H. & Yang, Y. L. Thermogravimetry of thermoplastic polyimide powders under four different atmospheres. *Macromol. Mater. Eng.* **286**, 421-428 (2001).

29. Musikabhumma, K. & Masuda, T. Synthesis and properties of widely conjugated polyacetylenes having anthryl and phenanthryl pendant groups. *J. Polym. Sci., Part A: Polym. Chem.* **36**, 3131-3137 (1998).

30. Bourbigot, S. & Flambard, X. Heat resistance and flammability of high performance fibres: a review. *Fire Mater.* **26**, 155-168 (2002).

31. Choi, S. W., Ohba, S., Brunovska, Z., Hemvichian, K. & Ishida, H. Synthesis, characterization and thermal degradation of functional benzoxazine monomers and polymers containing phenylphosphine oxide. *Polym. Degrad. Stabil.* **91**, 1166-1178 (2006).

32. Wang, M. C. & Zhao, T. Polyarylacetylene blends with improved processability and high thermal stability. *J. Appl. Polym. Sci.* **105**, 2939-2946 (2007).

33. Okuzaki, H. & Kubota, I. Electrical and mechanical properties of poly(*p*-phenylene) films prepared by electrochemical polymerisation. *Synth. Met.* **153**, 161-164 (2005).

Supplementary Information is linked to the online version of the paper at www.nature.com/nature.

Acknowledgements This work was supported by **the Royal Society, UK**.

Correspondence and requests for materials should be addressed to X.G.L.(adamxgli@yahoo.com) and M.G.M.(mark.moloney@chem.ox.ac.uk).